Available online at www.sciencedirect.com

Manufacturing Letters

Manufacturing Letters 00 (2021) 000–000

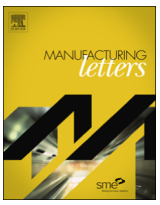

50th SME North American Manufacturing Research Conference (NAMRC 50, 2022)

Analyzing the evolution of tool wear area in trochoidal milling of Inconel 718 using image processing methodology

Ankit Agarwal[a,*], Nils Potthoff[b], Aash M Shah[a], Laine Mears[a], Petra Wiederkehr[b]

[a] *International Center for Automotive Research, Clemson University, Greenville, SC 29607*
[b] *Virtual Machining, TU Dortmund University, Otto-Hahn-Straße 12, 44227 Dortmund, Germany*

Abstract

Nickel-based superalloys belong to a category of material employed for extreme conditions and exhibit high strength properties at elevated temperatures that result in poor machinability. Machining such difficult-to-cut materials like Inconel 718 leads to a high rate of tool wear, and therefore trochoidal milling toolpath is used to improve productivity and tool life. The current study analyzes the evolution of the flank wear area of the tool during trochoidal milling of Inconel 718 using an image processing methodology. It is attempted by performing experimental studies until tool failure occurs at several cutting conditions. The machining is performed through several iterations on an identical cutting path, and the number of iterations to failure is recorded. The microstructural image of a flank wear area is captured upon each iteration and processed using an image processing algorithm. It is realized that the evaluation of flank wear area can be an effective parameter to analyze tool wear. Also, the image processing methodology works effectively and can be extended during real-time machining.

Keywords: Tool wear area; Trochoidal milling; Image processing; Inconel 718

1. Introduction

Tool wear is the primary source of multiple disturbances contributing to the deterioration of component accuracy during machining of nickel-based superalloys like Inconel 718 [1]. The monitoring and control of tool wear are imperative to avoid or minimize process disturbances such as vibrations, high cutting force, chatter, surface error, etc [2]. In addition, the reliable monitoring of tool wear assists process planners in the selection and adjustment of optimum machining parameters. The manufacturing industries are experiencing significant transformations in recent times due to the evolution of Industry 4.0. The newer set of technological solutions necessitate real-time monitoring of manufacturing processes using sensors followed by data analytics to evaluate the status and adjustment of parameters. It is necessary to have appropriate process knowledge embedded into the decision-making system to adjust machining parameters. In this context, the present research work attempts to automate the process of evaluating the wear area of the tool during machining of Inconel 718.

The literature presents several approaches to predict or monitor tool wear for various machining processes. These approaches can be broadly classified into two groups as indirect and direct approaches [3]. The indirect approaches aim to establish the relationship between process/cutting parameters and the different states of tool wear. The data of process parameters such as cutting force [4], vibrations [5], acoustic emission [6], temperature [7], surface roughness [8] is collected through multiple sensors and processed to generate a computational model that correlates process parameters with tool wear. The developed computational model is subsequently employed for predicting the state of tool wear. The real-time accumulation of data is easily accessible, but it has significant noise and outliers due to the process dynamics and characteristics of measuring sensors. The

* Corresponding author. Tel.: +1-864-990-8230.
E-mail address: agarwa3@clemson.edu (Ankit Agarwal).

presence of such elements yields poorly fitted correlation and lowers the prediction accuracy of the indirect approaches. Zhou and Xue [9] presented a review of indirect methods employed for monitoring and evaluating tool wear during the milling process.

The direct approaches aim to measure the tool wear implicitly during the machining process. An optical sensor, camera, or microscope is used to capture images of the tool, and then a change in the appearance, geometric shape, and surface properties is evaluated. With the advancements in high-speed cameras, the direct approaches are beneficial due to the high accuracy of measuring instruments, and they do not interfere during the machining process. However, real-time implementation of this approach is challenging due to existence of coolant and chips on surface of the tool. Kurada and Bradley [10] illuminated the flank wear area using fibre-optic light source and captured its reflected pattern using CCD camera during CNC turning. The image segmentation methodology was applied to estimate flank wear width. Lanzetta [11] presented an algorithm to recognize and classify the mode of wear (e.g., flank, crater, BUE, peening) and failure (e.g., catastrophic, thermal softening, chipping) of the cutting tool in turning and milling operation. Niranjan Prasad and Ramamoorthy [12] used stereo images and artificial neural network to visualize and evaluate flank wear in three dimensions. Zhang et al. [13] extracted edges of tool wear region through column-wise scanning of image to measure width of flank wear. The sub-pixel detection technology was applied to enhance the accuracy of results. Zhu et al. [14] applied morphological element analysis that segments the image in several regions and extract flank wear area during micro milling operation. The concept of digital image processing to measure wear width and area was further extended to drilling operation [15, 16]. Recently, Bergs et al.[17] applied a deep learning approach to classify the type of tool (end mill, drill, inserts) and evaluate tool wear area through microscopic images.

Based on the current literature review, it can be realized that monitoring of tool wear width has been studied considerably and assumed as a criterion for defining level of tool wear. However, the studies related to estimation of the wear area of the tool are limited to some operation and has not been investigated thoroughly, especially during trochoidal milling of difficult-to-machine materials. In the case of trochoidal milling, the linear path is superimposed on the rotational motion of the tool center point and has varying chip load along the cutting path. Also, during machining of difficult-to-machine materials the wear area is developed in intricate mechanical and thermal conditions. The compound effect of varying chip load and complex machining conditions suggests a need for a more comprehensive parameter such as the flank wear area of the tool as a criterion to define the state of tool wear. Generally, the measurement of the flank wear width is affected by human influence. In order to minimize this influence an automated detection of the flank wear area can help to provide a consistent evaluation quality. Therefore, the present study aims to develop an image processing-based methodology to estimate and monitor the flank wear area of the tool during trochoidal milling of Inconel 718. Further, the study also presents and analyzes the evolution of the flank wear area of the tool over the volume of material removed.

Henceforth, the paper is organized as follows; Section 2 outlines the details of the experimental setup and design of experiment used in the present study. Section 3 presents an overall framework for estimating the flank wear width and transforming the same into the flank wear area of the tool. Section 4 summarizes the experimental analysis of the flank wear area and its effect on cutting forces. The paper concludes with a summary of contributions and scope of future work from the present work in Section 5.

2. Experimental Design

2.1. Trochoidal Toolpath

The toolpath for trochoidal milling is controlled using three important parameters, (1) rotational speed of the tool (θ, RPM), (2) revolutionary motion of tool center ($\phi, rad/s$), and (3) step-over feed rate ($v, mm/s$) in the direction of linear motion. The X- and Y- coordinates for the trajectorial motion of the tool tip are expressed using Eqs. (1) and (2) and depicted in Fig. 1, where S_w, R_c, t represents slot width, radius of the cutter, and time respectively. In Eqs. (1) and (2), ϕ is a function of feed rate (mm/s) and evaluated using Eq. (3).

$$X_c = (\frac{S_w}{2} - R_c)\ cos(\phi t) + R_c\ cos(\theta t) \tag{1}$$

$$Y_c = (\frac{S_w}{2} - R_c)\ sin(\phi t) + R_c\ sin(\theta t) + vt \tag{2}$$

$$\phi = Feed\ rate\ /\ (\frac{S_w}{2} - R_c) \tag{3}$$

2.2. Machining and wear image capturing setup

The experiments were performed on a 3-axis vertical milling machine (OKUMA Genos M560-V) using a 2-flute indexable end mill and Inconel 718 workpiece material, as shown in Fig. 2a). Table 1 summarizes the attributes related to the tool and workpiece used during experimentation. All the experiments

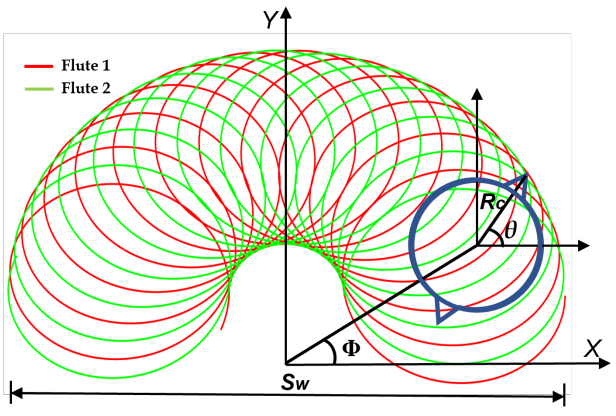

Fig. 1. Trochoidal toolpath for 2-flute cutter

were carried out with Sandvik Coromill Shoulder Mill Cutter of 15.875 *mm* diameter and RA390-11 T3 08M-PL S30T carbide inserts having multilayer TiAlN coating. The workpiece used was cylindrical blocks of Inconel 718 with a diameter and length of 50.8 mm and 76.2 mm. A table-mounted piezoelectric dynamometer (Kistler 9257B) was used to measure the cutting forces. The signals measured through a dynamometer were amplified and recorded using the Kistler data acquisition system and Dynoware software. The machinist vice was mounted on the dynamometer to secure the workpiece. The machinist vise ensures that pressure is applied downward onto the workpiece, eliminating the chance of the workpiece being pushed upward. The fixture was developed to hold the round shape workpiece that makes contact at four points along the half contour of the workpiece, as shown in Fig. 2b). The microstructure images of the tool wear were captured using the ZEISS Axio Vert.A1 vertical microscope depicted in Fig. 2c). The vertical microscope has a light source on the bed and has different lenses, which was used depending upon the necessary zoom. A hollow cylinder stand was prepared to mount the tool over the vertical microscope. The tool as a whole was placed on a hollow cylinder to capture the microstructure image of the carbide inserts.

2.3. Design of Experiment (DoE)

Table 2 outlines the DoE used to study effect of surface speed parameter on flank wear area of the tool and cutting force during trochoidal milling of Inconel 718. The trochoidal slots of 40 mm width were machined during each test for the comparison of results. The surface speed was varied in the range of 25-60 m/min, and feed per tooth was maintained constant at 0.25 mm/tooth. The progression of flank wear area and its effect on cutting forces were analyzed by machining the slot iteratively at an axial depth of cut of 1 mm in each iteration. The new inserts were used for each test, and the number of iterations required for the tool's failure was recorded. The cutting force and tool wear images were recorded at each iteration. The volume of material removed in each iteration was 842.4 mm^3. The material was machined along the axial dimension of the circular workpiece to have consistent material properties while changing the block of material. To study the fully engaged trochoidal milling and isolate the effects of interrupted cuts in the trochoidal path, the initial section of the slot was cleared using another tool, as shown in Fig. 3. The distance between the top of the workpiece and the vice block for every test pass was held constant by employing the following procedure. Initially, upon completion of every test pass, the workpiece was approximately raised slightly above the initial position using a measuring gauge. Thereafter, the revised origin and height of the repositioned workpiece were measured using an On-Machine Measuring (OMM) probe. Finally, a facing operation was performed to ensure the exact distance between the workpiece and vice. It removes the leftover material of the previous iteration and any extra material due to repositioning of the workpiece.Due to the application of the OMM probe, the process was repeatable. Also, the facing operation ensured that the scrap material was removed before the next iteration. The flood coolant type was applied to remove the heat generated at the cutting zone with the help of flexible pipes, having a concentration of 8.5%.

Table 1. Tool and Workpiece Attributes

Tool Attributes (Carbide Indexable End Mill)		
Manufacturer	:	Sandvik
Catalog Code (Holder)	:	RA390-016EH16-11L
Catalog Code (Insert)	:	RA390-11 T3 08M-PL S30T
Cutter Diameter	:	15.875 mm
Helix Angle	:	30°
Lead Angle	:	90°
No. of Flutes	:	2
Flute Length	:	10 mm
Coating	:	TiAlN
Workpiece Attributes		
Material	:	Inconel 718
Workpiece Shape	:	Round
Diameter	:	50.8 mm
Length	:	76.2 mm

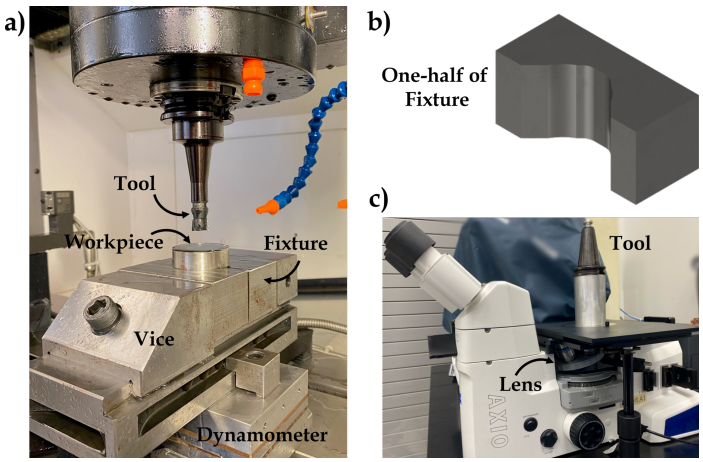

Fig. 2. Experimental setup; (a) Machining setup for trochoidal milling, (b) One-half of a fixture, and (c) Vertical microscope to capture tool wear images

Table 2. Design of Experiments

Test No.	Surface Speed (m/min)	Spindle Speed (RPM)	Iteration Completed
1	25	501	25
2	45	902	14
3	60	1203	11

Step over feed rate (v)	:	0.25 mm/s
Axial Depth of Cut	:	1 mm
Feed per Tooth	:	0.25 mm/tooth
Slot Width	:	40 mm
Volume Removed per Iteration	:	842.4 mm^3
Coolant Flow	:	Flood
Coolant Concentration	:	8.5 %

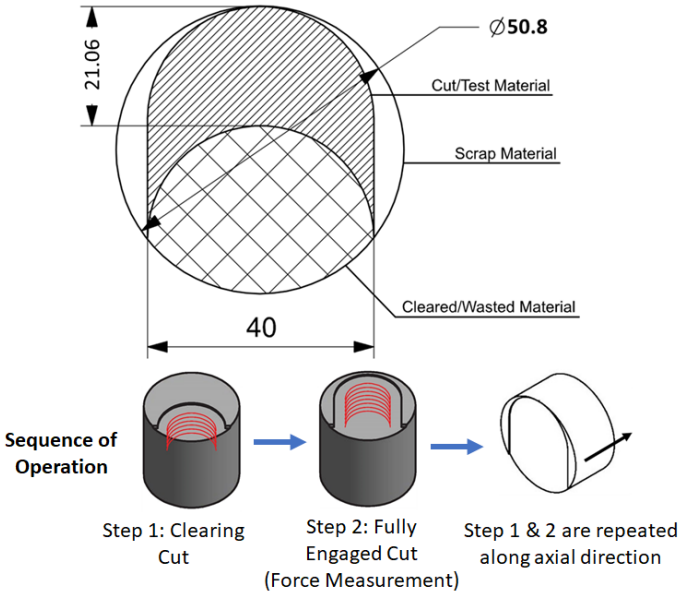

Fig. 3. Workpiece attributes and Sequence of operation

3. Methodology for measurement of flank wear area

The framework for estimating the flank wear area of the tool proposed in this research work is based on an image processing program developed using MATLAB software. The step-wise procedure is illustrated subsequently in this section using a representative example of a tool wear image depicted in Fig. 4. Firstly, the image captured through a microscope is preprocessed to filter noise and actual wear area of interest. Secondly, the cutting edge of the tool is extracted to have a reference for measurement. Finally, the width and area of flank wear is measured along the cutting edge of the tool.

3.1. Image preprocessing

The microstructural image (Fig. 4a)) captured using the Zeiss Axiovision software is cropped precisely, and brightness/contrast levels are altered to better visualize the flank wear area of the tool, as shown in Fig. 4b). The obtained image contains various noisy features (region other than tool wear) that interfere with the subsequent process of extracting flank wear area. Therefore, the image is further processed to eliminate noise using a Gaussian filter. The Gaussian filter smoothens the image by averaging out any rapid changes in the pixel's intensity. The smoothening operation assists in removing outlier pixels or noise in the image while preserving the edges and other properties of the image intact, as shown in Fig. 4c). Thereafter, the image is binarized using Otsu's approach [18], which follows an adaptive thresholding process to determine the best threshold value for an input image by running over all potential threshold values (0 to 255). The pixels with intensity values less than the threshold value are replaced as zero's (black) while turning all other values to one's (white), as depicted in Fig. 4d).

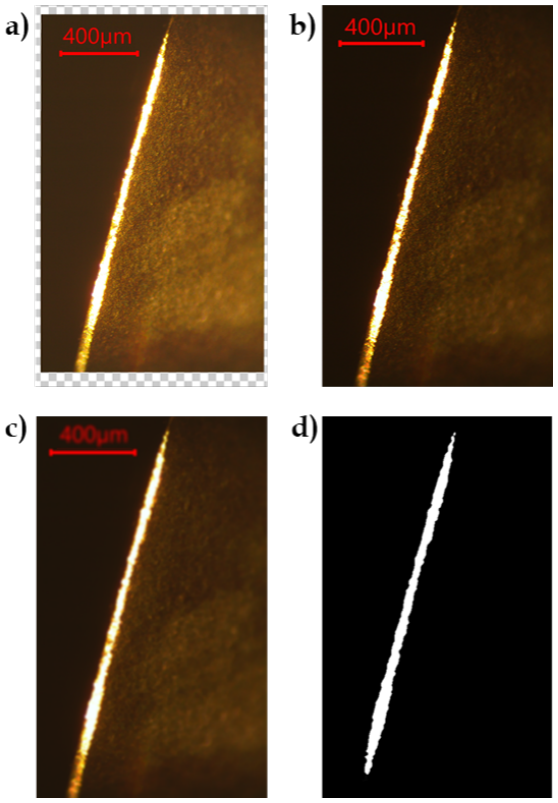

Fig. 4. Preprocessing of tool wear image; (a) Captured image, (b) Crop and brightness adjustment, (c) Image smoothening, and (d) Binarized image

3.2. Detection of tool cutting edge

The binarized image (Fig. 4d)) generated using image preprocessing is further analyzed to detect the tool's cutting edge by applying the Standard Hough Transform (SHT) algorithm [19]. The application of the SHT algorithm necessitates identifying the boundary of the flank wear area that will be used as an input for the algorithm. The present research work uses Canny edge detection [20] to locate the boundary of the flank wear in a binarized image. It outputs the curve that follows a path of a drastic change in the intensity/brightness value of the image. The Canny edge detection method returns a binary image with a pixel intensity value of one where a boundary is identified and zero at other pixel locations, as shown in Fig. 5a). The SHT algorithm applies the parametric equation of a line ($l = x\,cos(\alpha) + y\,sin(\alpha)$) which passes through the origin and is normal to the cutting edge of the tool. The algorithm outputs length (l) of the normal line and angle (α) between the normal line and the X-axis. However, the detected cutting edge of the tool is of infinite length and requires further analysis. It is accomplished by checking the pixel intensity value along the detected cutting edge to determine its endpoints. Also, to connect the cutting edge through the black portions, the following constraints were defined; (1) search for endpoint (intensity value equal to one) in the range of 50 pixels with zero intensity value and (2) length of the cutting edge as 1400 μm. The detected cutting edge of the tool is depicted in Fig. 5b).

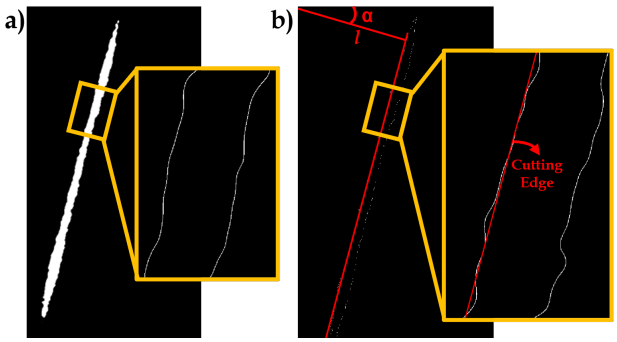

Fig. 5. Detection of tool cutting edge; (a) Boundary of tool wear zone and (b) Cutting edge

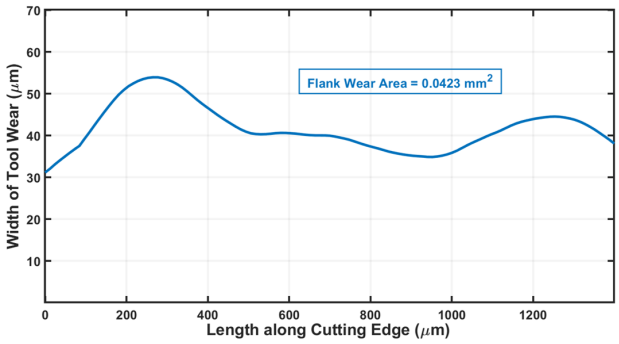

Fig. 7. Width of tool wear and flank wear area along cutting edge

3.3. Evaluation of flank wear area

Once the zone of wear area and tool's cutting edge is identified, the next step is to evaluate the flank wear area of the tool. Firstly, the tool's cutting edge is discretized into numerous sections of equal length, and perpendicular lines are plotted through each section, as shown in Fig. 6. Secondly, the number of pixels with a value equal to one (white) is calculated for each perpendicular line on either side of the cutting edge. The methodology uses Optical Character Recognition (OCR) [21] to identify the scale value in the image and then search for a scale bar line to evaluate the length between two pixels. Lastly, the width of the tool wear is assessed at each section along the cutting edge by converting pixel measurement into a metric unit (μm) of length. Thereafter, trapezoidal integration is applied to evaluate the flank wear area up to the tool cutting edge of 1400 μm from the tool tip as depicted in Fig. 7.

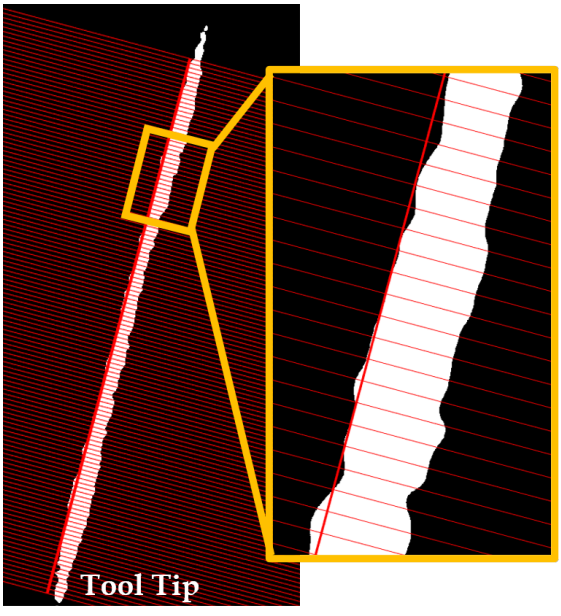

Fig. 6. Discretization of tool cutting edge and plotting of perpendicular lines

The literature has reported that tool wear directly influences the machining quality of the manufactured components and needs to be evaluated accurately for determining the useful life of a tool. Conventionally, the flank wear width of the tool is calculated manually by comparing the width of the flank wear zone with the scale bar of an image. The process is repeated at different locations along the cutting edge to evaluate the flank wear area of the tool. This procedure is time-consuming and induces errors due to the involvement of manual measurements and interpolation. The developed methodology in this section for evaluating the flank wear area of the tool is easier to use, more accurate, and less time-consuming. It also reduces human efforts for assessing flank wear width and wear area along the cutting edge.

4. Analysis of flank wear area and cutting force

4.1. Analysis of flank wear area

The methodology outlined in Section 3 for measuring the wear area of the tool has been applied to evaluate and analyze the progression of flank wear area of the tool during trochoidal milling of Inconel 718 under cutting conditions listed in table 2. Figure 8 represents the qualitative evolution of flank wear on the carbide insert used in test 3, where tool failure can be observed during the 12^{th} iteration. Also, the experimental results depict the flank wear and chipping as the dominant mode of tool wear and failure, respectively.

Fig. 9 represents the quantitative progression of flank wear area of the tool over the volume of material removed before tool failure for all cutting conditions listed in Table 2. The machining at a higher surface speed (60 m/min – test 3) rapidly evolves flank wear area due to higher chip load and temperature. In comparison, gradual or slower evolution of flank wear area is observed at a lower surface speed (25 m/min – test 1). It can be concluded that lower values for surface speed assist in enhancing the behaviors of wear area evolution. Also, the curves presenting the tool's flank wear area to volume of material removed can be classified into three different regions, namely (a) initial region, (b) steady-state region, and (c) failure region. In the initial region, the flank wear area increases rapidly in the form of an exponential curve. It remains for a very short period and occurs up to approximately in the range of 1685 – 2525 mm^3 (2-3 iteration) volume of material removal in each test. The

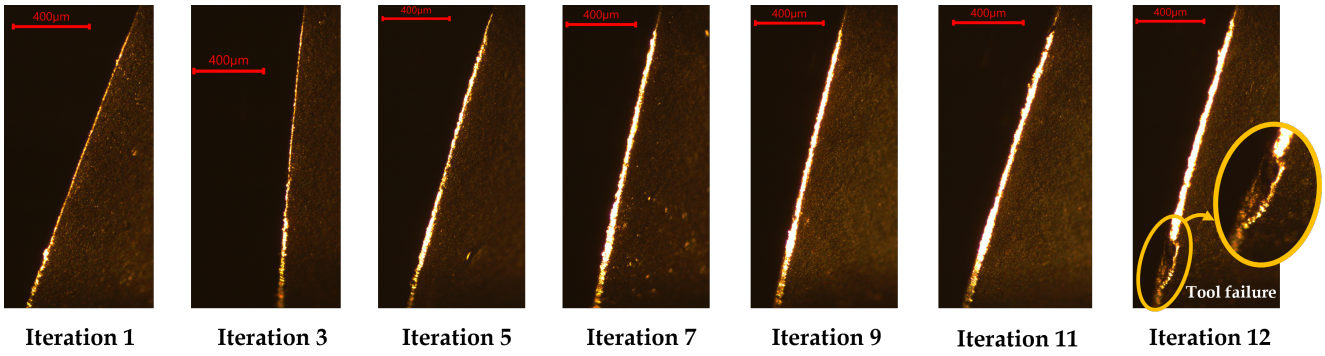

Fig. 8. Qualitative evolution of tool wear area (Test 3)

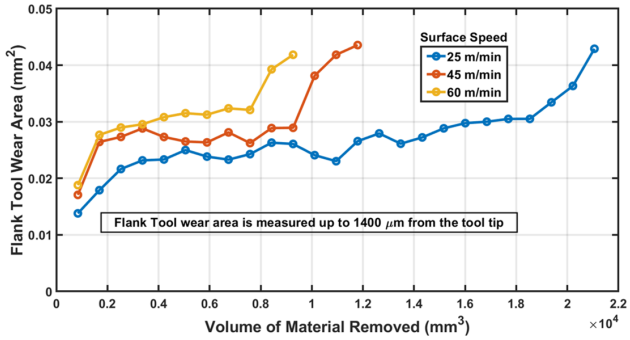

Fig. 9. Quantitative evolution of flank tool wear area for different surface speed

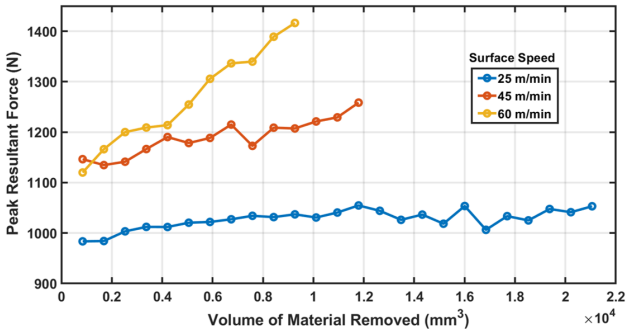

Fig. 10. Comparison of peak resultant force for different surface speed

steady-state region corresponds to an intermediate state where a gradual increase of flank wear area is observed. The rate of growth in flank wear area was nearly constant until region to tool failure (0.03 – 0.045 mm^2) was reached. The amount of material removed in this stage decreases with an increase in surface speed. The flank wear area increases drastically in the failure region, and the chipping mode of tool failure is observed at ≈ 0.045 mm^2.

4.2. *Cutting force analysis*

The machining of Inconel 718 results in rapid work hardening, and it becomes more difficult for further machining. Also, with an increase in material removal, the wear area of the tool evolves, and blunting of tool cutting edge occurs. The effect of both factors leads to the plowing/rubbing action of material removal instead of shearing. The combined phenomenon of work hardening and tool wear results in higher cutting force and temperature. Fig. 10 represents the resultant peak force over the volume of material removed at different surface speeds during trochoidal slot milling of Inconel 718. It has been observed that the peak value of resultant force increases with the volume of material removed, which is a well-understood phenomenon that is attributed to the evolution of the flank wear area of the tool. The rate of increase in force values varies with the surface speed. The machining at a higher surface speed (60 m/min – test 3) shows higher variation in the force values, which correlates to the higher flank wear area. On the contrary, the lower variation in the force values is observed during lower surface speed (25 m/min – test 1) which can be interpreted to lower evolution rate of flank wear area. However, it can be realized that the overall trend of cutting forces increases with the volume of material removed, which complies with the trend at other higher speeds.

5. Conclusion and future work

This paper presented an image recognition-based method to measure the flank wear area of the tool during trochoidal milling of Inconel 718. The proposed method was implemented in the form of an automated computational program, and a series of experiments were performed to analyze the progression of the flank wear area of the tool over the volume of material removed. Based on the outcomes of the present study, it has been realized that the image processing method presented in this study can evaluate the flank wear width and wear area accurately and efficiently. Also, the proposed methodology was able to replicate the well-known curve of flank wear area versus the volume of material removed.

In future research work, the proposed method will be adopted for CNC machines during real-time machining. An image acquisition area consisting of optical and electrical hardware shall be set up inside the machine tool as a tool wear inspection station. The cutting tool will be positioned under the camera or lens that will be oriented to measure the tool's flank or other wear. In this regard, the positioning and orientation of the tool over the microscope lens will be analyzed for better capturing of wear images. The knowledge assessed will be transferred to the controller of

CNC machines to employ suitable tool wear compensation. Due to the development stage of the algorithm, it will be improved in further investigations.

Acknowledgements

The investigations are based on the research project "Stochastic Modeling of the Interaction of Tool Wear and the Machining Affected Zone in Nickel-Based Superalloys and Application in Dynamic Stability", which is kindly funded by the National Science Foundation under Grant No. 1760809 and the German Research Foundation (DFG – 400845424). Any opinions, findings, and conclusions or recommendations expressed in this material are those of the authors and do not necessarily reflect the views of the National Science Foundation.

References

[1] Wang, B., Liu, Z., 2018. Influences of tool structure, tool material and tool wear on machined surface integrity during turning and milling of titanium and nickel alloys: a review. The International Journal of Advanced Manufacturing Technology 98, 1925–1975.
[2] Chen, X., Li, H., 2009. Development of a tool wear observer model for online tool condition monitoring and control in machining nickel-based alloys. The International Journal of Advanced Manufacturing Technology 45, 786–800.
[3] Jeon, J., Kim, S.W., 1988. Optical flank wear monitoring of cutting tools by image processing. Wear 127, 207–217.
[4] Kaya, B., Oysu, C., Ertunc, H.M., 2011. Force-torque based on-line tool wear estimation system for cnc milling of inconel 718 using neural networks. Advances in Engineering Software 42, 76–84.
[5] Yuqing, Z., Xinfang, L., Fengping, L., Bingtao, S., Wei, X., 2015. An online damage identification approach for numerical control machine tools based on data fusion using vibration signals. Journal of Vibration and Control 21, 2925–2936.
[6] Jemielniak, K., Arrazola, P., 2008. Application of ae and cutting force signals in tool condition monitoring in micro-milling. CIRP Journal of Manufacturing Science and Technology 1, 97–102.
[7] Kim, S., Lee, C., Lee, D., Kim, J., Jung, Y., 2001. Evaluation of the thermal characteristics in high-speed ball-end milling. Journal of Materials Processing Technology 113, 406–409.
[8] Dutta, S., Kanwat, A., Pal, S., Sen, R., 2013. Correlation study of tool flank wear with machined surface texture in end milling. Measurement 46, 4249–4260.
[9] Zhou, Y., Xue, W., 2018. Review of tool condition monitoring methods in milling processes. The International Journal of Advanced Manufacturing Technology 96, 2509–2523.
[10] Kurada, S., Bradley, C., 1997. A machine vision system for tool wear assessment. Tribology International 30, 295–304.
[11] Lanzetta, M., 2001. A new flexible high-resolution vision sensor for tool condition monitoring. Journal of Materials Processing Technology 119, 73–82.
[12] Prasad, K.N., Ramamoorthy, B., 2001. Tool wear evaluation by stereo vision and prediction by artificial neural network. Journal of Materials Processing Technology 112, 43–52.
[13] Zhang, J., Zhang, C., Guo, S., Zhou, L., 2012. Research on tool wear detection based on machine vision in end milling process. Production Engineering 6, 431–437.
[14] Zhu, K., Yu, X., 2017. The monitoring of micro milling tool wear conditions by wear area estimation. Mechanical Systems and Signal Processing 93, 80–91.
[15] Su, J., Huang, C., Tarng, Y., 2006. An automated flank wear measurement of microdrills using machine vision. Journal of Materials Processing Technology 180, 328–335.
[16] Yu, J., Cheng, X., Lu, L., Wu, B., 2021. A machine vision method for measurement of machining tool wear. Measurement , 109683.
[17] Bergs, T., Holst, C., Gupta, P., Augspurger, T., 2020. Digital image processing with deep learning for automated cutting tool wear detection. Procedia Manufacturing 48, 947–958.
[18] Otsu, N., 1979. A threshold selection method from gray-level histograms. IEEE transactions on systems, man, and cybernetics 9, 62–66.
[19] Duda, R.O., Hart, P.E., 1972. Use of the hough transformation to detect lines and curves in pictures. Communications of the ACM 15, 11–15.
[20] Canny, J., 1986. A computational approach to edge detection. IEEE Transactions on pattern analysis and machine intelligence PAMI-8, 679–698.
[21] Bunke, H., Wang, P.S., 1997. Handbook of character recognition and document image analysis. World scientific.